Biol. Chem., Vol. 390, pp. 693–699, August 2009 • Copyright © by Walter de Gruyter • Berlin • New York. DOI 10.1515/BC.2009.090

Review

Structural and functional aspects of the multidrug efflux pump AcrB

Thomas Eicher[1], Lorenz Brandstätter[1] and Klaas M. Pos[2,*]

[1] Institute of Physiology and Zurich Center for Integrative Human Physiology (ZIHP), University of Zurich, Winterthurerstrasse 190, CH-8057 Zurich, Switzerland

[2] Cluster of Excellence Frankfurt – Macromolecular Complexes and Institute of Biochemistry, Goethe University Frankfurt, Max-von-Laue-Str. 9, D-60438 Frankfurt/Main, Germany

* Corresponding author
e-mail: pos@em.uni-frankfurt.de

Abstract

The tripartite efflux system AcrA/AcrB/TolC is the main pump in *Escherichia coli* for the efflux of multiple antibiotics, dyes, bile salts and detergents. The inner membrane component AcrB is central to substrate recognition and energy transduction and acts as a proton/drug antiporter. Recent structural studies show that homotrimeric AcrB can adopt different monomer conformations representing consecutive states in an allosteric functional rotation transport cycle. The conformational changes create an alternate access drug transport tunnel including a hydrophobic substrate binding pocket in one of the cycle intermediates.

Keywords: AcrB; alternate access transport mechanism; antibiotic resistance; binding change mechanism; drug transport; membrane protein structure; multiple drug efflux pump.

Introduction

Resistance of bacteria towards antibiotics is known to be evoked by at least three different mechanisms: (i) target modification [e.g., resistance against macrolides mediated by methylation of the ribosome (Skinner et al., 1983; Zalacain and Cundliffe, 1989, 1990) or resistance against fluoroquinolones by mutations in DNA gyrase (Yoshida et al., 1990; Hooper, 1995)]; (ii) antibiotic modification (e.g., hydrolysis of β-lactam ring by β-lactamase; Thomson and Smith Moland, 2000) or phosphorylation, adenylation or acetylation of aminoglycosides (Wright, 1999); and (iii) reduced accumulation of antibiotics in the target compartments (periplasm, cytoplasm) through suppression of porin synthesis (Hancock and Brinkman, 2002) and/or overproduction of efflux pumps (Nikaido, 1998, 2009; Lomovskaya et al., 1999; Li and Nikaido, 2004; Lomovskaya and Totrov, 2005; Nikaido and Takatsuka, 2008).

Resistance conferred by antibiotic and target modification is often restricted to a single class of antibiotics or even a single compound. In contrast, multidrug resistance (MDR) transporters enable the bacteria to efflux a broad range of substances and hence confer simultaneous resistance to unrelated compounds. The central role of MDR transporters as a primary line of defense and, intriguingly, as mediators for the acquisition of other resistance mechanisms have been shown in several cases (Lomovskaya et al., 1999; Mazzariol et al., 2000; Mahamoud et al., 2007).

Proteins of the Resistance-Nodulation-Division (RND) superfamily (TC#2.A.6) are ubiquitous in all phyla. In prokaryotes, their main physiological function seems to be associated with the extrusion of noxious substrates, with notable exceptions such as the secretory accessory proteins SecDF (Gardel et al., 1987; Pogliano and Beckwith, 1994), lipid exporter MmpL7 (Camacho et al., 2001; Domenech et al., 2005) and the putative lipooligosaccharide nodulation factor exporter NolG (Baev et al., 1991). In Eukarya, however, the functionally characterized RND proteins seem to be involved in lipid homeostasis (Davies et al., 2000; Davies and Ioannou, 2000; Sleat et al., 2004; Infante et al., 2008a,b) and cell morphogenesis (Taipale et al., 2002; Nakano et al., 2004). As phylogenetic analyses suggest, energization via the proton (or sodium ion) motive force might be a common feature for all RND proteins (Saier and Paulsen, 2001).

Resistance nodulation division (RND) efflux pump AcrB

Proteobacterial members of the RND superfamily are located in the inner membrane. They typically assemble with two accessory proteins, a membrane fusion protein (MFP; TC#8.A.1) and an outer membrane factor (OMF; TC#1.B.17). The so-formed tripartite MFP/RND/OMF complex spans the inner membrane, the periplasm as well as the outer membrane of the Gram-negative bacterium. Most extensively studied examples of these three component systems are MexA/MexB/OprM of *Pseudomonas aeruginosa* or AcrA/AcrB/TolC of *Escherichia coli* (Figure 1A). Both outer membrane and tripartite efflux pumps are considered to be the main barrier for drugs on their way to the inside of the bacterial cell (Plesiat and Nikaido, 1992; Nikaido, 2003, 2009). It is this combination of the intrinsic impermeability of the outer membrane, reduction of the number of outer membrane pores and upregulation of multidrug efflux pumps which enables effective synergistic drug resistance (Nikaido,

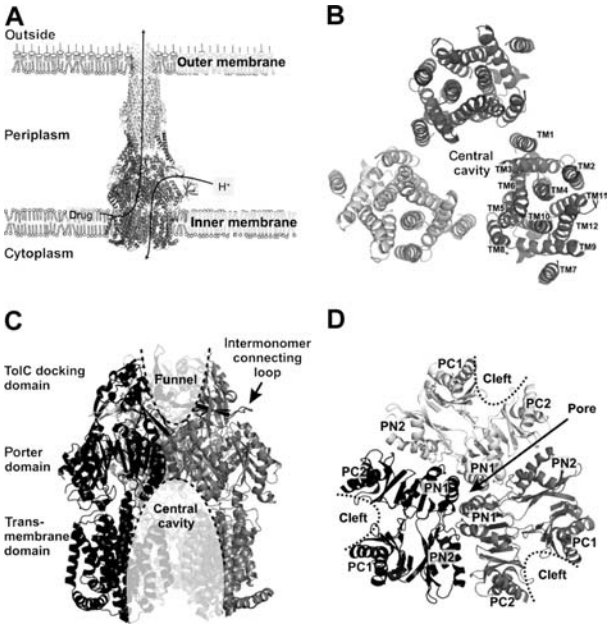

Figure 1 Schematic drawing of the tripartite multidrug efflux system AcrAB-TolC of Gram-negative *E. coli* and AcrB structural features.
(A) The inner membrane component AcrB (RND component) accounts for substrate recognition/selection and energy transduction. Drugs might be captured from the outer leaflet of the inner membrane and are extruded in a coupled exchange with protons. The TolC channel (OMF component) mediates the exit through the outer membrane and connects to AcrB via a long periplasmic conduit. AcrA (MFP component) connects AcrB and TolC. The presence of all three components is essential for the MDR phenotype. (B) Topological view of the transmembrane (TM) domain perpendicular to the membrane plane. TM4 and TM10 are surrounded by the other 10 TM helices. The TM domains of the three monomers confine a large central cavity. (C) Side view of trimeric AcrB. A central pore located in the porter domain separates a funnel-like structure in the TolC-docking domain from the central cavity located in the TM domain. The central pore, however, does not appear to allow direct passage of drugs. The trimeric state of AcrB is mainly stabilized by the intermonomer connecting loops. (D) Top view of the porter domain with its subdomains PN1, PN2, PC1 and PC2 perpendicular to the membrane plane. The central pore is formed by three α-helices, donated by the PN1 subdomains of each AcrB monomer. A cleft is apparent between the PC1 and PC2 subdomains of each monomer.

1996). Strikingly, dysfunction of only one component of the tripartite system results in a complete drug-sensitive phenotype.

RND proteins, such as MexB (Mex: multiple efflux) and AcrB (Acr: acriflavine resistance), represent the energy module and the substrate specificity determinant of the tripartite RND/MFP/OMF efflux system. The substrate variety of MexB or AcrB, compared to the many other MDR proteins, is staggering. It includes dyes, bile salts, organic solvents and antibiotics of different chemical classes; molecules that are anionic, cationic, zwitterionic, aromatic or just aliphatic; chemicals of bulky or planar geometry. However, since export of membrane lipids and co-factors, such as flavins, is expected to be detrimental for bacterial cells, additional criteria to discriminate between noxious compounds and vital cell constituents must exist, a matter of ongoing research. Like most proteobacterial RND proteins, AcrB consists of 12 transmembrane (TM) α-helices and two extensive periplasmic loops which account for approximately half of the 1049 amino acids of the protein. The loops connect TM1 with TM2 and TM7 with TM8, respectively. The topology of the TM domain – five-plus-one-TM helices, repeated twice – is also referred to as RND signature (Ioannou, 2001). The repetition of the motif suggests that RND transporters arose as a result of an intragenic tandem duplication event.

It appears that the substrate specificity determination is residing in the periplasmic loops, which was shown through the design of chimeric proteins. Specifically, the two extracellular loops of the *Escherichia coli* aminoglycoside exporter AcrD were replaced by the periplasmic loops of AcrB (Elkins and Nikaido, 2002). The resulting transporter exhibited a resistance pattern that was typical for AcrB. Conversely, when the periplasmic loops of AcrB were replaced by the corresponding domains of AcrD, the chimeric protein lost the ability to confer resistance towards substrates of AcrB, but the resistance towards aminoglycosides was enhanced. Domain swapping experiments between MexB and MexY led to similar results (Eda et al., 2003). Here, the periplasmic loops of MexB were combined with the TM domain of MexY. Again, the resulting protein conferred resistance towards typical MexB substrates, while the cells were susceptible towards MexY specific drugs. Additional evidence on the role of the periplasmic domain in substrate specificity determination came from a study where six single site mutations causing altered substrate specificity were all found to be located on the extracellular loops (Mao et al., 2002). Crystallographic studies provided further insights on the role of the periplasmic loops in substrate recognition and transport (Murakami et al., 2006; Seeger et al., 2006; Sennhauser et al., 2007).

Structure of AcrB

The first AcrB structure (Murakami et al., 2002) was based on 3.5 Å X-ray diffraction data from crystals containing one unliganded AcrB monomer in the asymmetric unit and for which the trimer is generated by exact crystallographic symmetry. Each monomer contains a TM domain with 12 TM helices which form a bundle with two central helices (TM4 and TM10) in its topological core. On these central α-helices, three titratable residues, Asp407, Asp408 and Lys940, were found to be essential for protein function (Guan and Nakae, 2001; Su et al., 2006; Takatsuka and Nikaido, 2006; see Figure 1B).

The periplasmic part – formed by the periplasmic loops described above – extends 70 Å into the periplasm. It can be further divided into a TolC docking domain which is most distal from the membrane plane and a porter domain, formerly known as pore domain (Figure 1C).

The TolC-docking domain is the expected interaction site of the outer membrane channel TolC (Tikhonova and Zgurskaya, 2004; Tamura et al., 2005; Bavro et al., 2008; Pietras et al., 2008). The TolC docking domain of each monomer furthermore exhibits a hairpin-like loop that protrudes into the neighboring monomer, which appears

to be the main stabilizing factor for the trimeric AcrB complex.

The porter domain is divided into subdomains PN1, PN2, PC1 and PC2, which are coupled by sequential proximity (PN1–PN2, PC1–PC2) or by sharing β-strands to form common β-sheets (PN2–PC1, PC2–PN1; see Figure 1D). The PN1 subdomains are located in the center of the trimer, surrounded by the PN2, PC1 and PC2 subdomains towards the periphery. A cleft is apparent between the PC1 and PC2 subdomains, which is approximately perpendicular to the membrane plane. In the center of the trimer, the TolC docking domain exhibits a funnel-like structure narrowing to a central pore, defined by α-helices (designated pore helices) of the PN1 subdomains of each monomer. This pore has a small diameter and therefore does not allow drug passage in this conformation. Towards the membrane plane, the central pore leads to a central cavity and further to a 30–35 Å wide, presumably lipid-filled TM hole defined by the ring-like arrangement of the TM helices of the trimer. Three vestibules at the monomer interface located just above the membrane plane lead towards the central cavity. It is postulated that substrate might access the central cavity via these vestibules (Murakami et al., 2002). Indeed, there have been several reports on AcrB/substrate co-crystals with positive densities in the electron density maps derived from (symmetric) R32 crystals that have been interpreted as substrate molecules bound to the inner wall of the AcrB central cavity (Yu et al., 2003a,b, 2005; Pos et al., 2004; Tornroth-Horsefield et al., 2007; see Figure 1B, C).

In 2006 and 2007, three groups independently published an asymmetric structure of AcrB grown in the monoclinic space group C2 (2.8–2.9 Å; Murakami et al., 2006; Seeger et al., 2006), triclinic space group P1 (3.0 Å; Seeger et al., 2006) and an AcrB structure including bound designed ankyrin repeat proteins (DARPins) grown in orthorhombic space group $P2_12_12_1$ (2.5 Å; Sennhauser et al., 2007). The DARPin bound AcrB structure was almost identical with the AcrB structures crystallized without binder with root mean square deviation (rmsd) of the superimposed trimeric structures ≤ 1 Å. The DARPin molecules only bind to the loose and the tight conformers, resulting in a ratio of two DARPin molecules per AcrB trimer. This stoichiometry was verified by sedimentation velocity experiments, suggesting that in solution and probably also *in vivo* AcrB adopts mainly the asymmetric conformation (Sennhauser et al., 2007).

Within the asymmetric AcrB trimer, each monomer has a different conformation denoted as loose, tight and open (access, binding and extrusion, respectively; Murakami et al., 2006; Seeger et al., 2006), while the loose state is closest to the conformation of the monomers in the symmetric structure (Murakami et al., 2002). Although the pore helices are differently oriented in the asymmetric structure as compared to the symmetric structure, the pore diameter is similar and hence there does not appear to be a substrate export pathway through the pore. Instead, conformer specific cavities and tunnels could be identified in the porter domain (Murakami et al., 2006; Seeger et al., 2006; Sennhauser et al., 2007; see Figure 2). In the loose conformer, a tunnel (tunnel 2) starts in the PC1/PC2 subdomain cleft approximately 15 Å above the membrane plane and protrudes in the direction of the pore. In the tight conformer, an additional tunnel (tunnel 1) with an entrance situated in a groove formed by TM8 and TM9 at the height of the membrane plane is apparent. Due to reorientation of the PN2 subdomain in the tight monomer, a hydrophobic pocket at the interface of PN2 and PC1 subdomains is created (Figure 2). This pocket is situated close to the end of tunnels 1 and 2 in the tight conformer (defined by the PN1 subdomain of the adjacent open monomer) and is rich in aromatic amino acids (Bohnert et al., 2008), a feature that is often observed for binding pockets of MDR proteins (Zheleznova et al., 1999; Schumacher et al., 2001, 2004; Murray et al., 2004; see Figure 2, inset). Indeed, Murakami et al. (2006) detected electron densities for the AcrB sub-

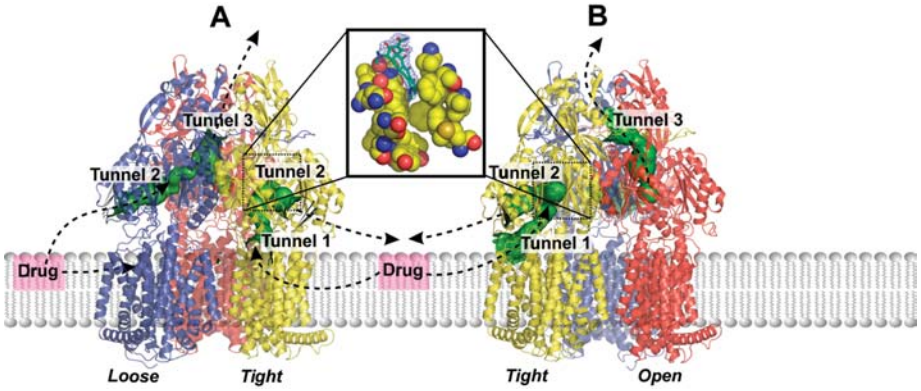

Figure 2 Tunnels in the porter domain of trimeric AcrB peristaltic drug efflux pump.
The AcrB monomers are presented in blue (loose), yellow (tight) and red (open). The tunnels are highlighted as green surfaces in a ribbon model of the AcrB trimer and might function as transport paths of drugs. Tunnel 1 might serve as entrance for drugs from the outer leaflet of the inner membrane towards the hydrophobic substrate binding pocket. Tunnel 2 might serve as an alternative entrance for substrates entering via the periplasm or as an exit duct for non-substrates. Tunnel 3 in the *open* monomer is the exit pathway for substrates towards TolC and the outside medium. Inset: in the T monomer (yellow), a hydrophobic pocket is defined by phenylalanine, valine, isoleucine and tyrosine side chains at the PN2/PC1 interface. Bound minocycline is depicted with the observed electron density in a $2F_o$-F_c electron density map contoured 1 σ (T. Eicher, M. Seeger, K.M. Pos and colleagues, unpublished data). Panels (A) and (B) represent in each case a one-third conversion of a full L→T→O→L cycle [adapted from Pos (2009) and modified].

strates minocycline and doxorubicin in the hydrophobic pocket. By using a brominated derivative of the former compound (9-bromo-minocyclin), they unambiguously could assign the position of this substrate within the binding pocket. In the open monomer, the lateral periplasmic entrance of the tunnel observed in the loose and tight conformation is now closed owing to coil-to-helix transition of TM8, whereas another tunnel (tunnel 3) is created due to tilting of the pore helix (PN1 subdomain). The latter tunnel leads from the now collapsed binding pocket to the funnel located in the center of the AcrB trimer (Figure 2).

Transport mechanism

It is postulated (Murakami et al., 2006; Seeger et al., 2006, 2008b; Sennhauser et al., 2007; Murakami, 2008; Pos, 2009) that substrate transport by AcrB is accomplished via functional rotation in which each monomer changes its conformation in a concerted fashion (Figure 3). The mechanism resembles that of Boyer's binding change mechanism of the F_1F_o ATPase, where conformational cycling of the (α and) β subunits through the states loose, tight and open leads to the synthesis of ATP (Hackney et al., 1979; Hutton and Boyer, 1979; Boyer, 1997).

One transport hypothesis assumes the substrates to be garnered from the outer leaflet of the inner membrane

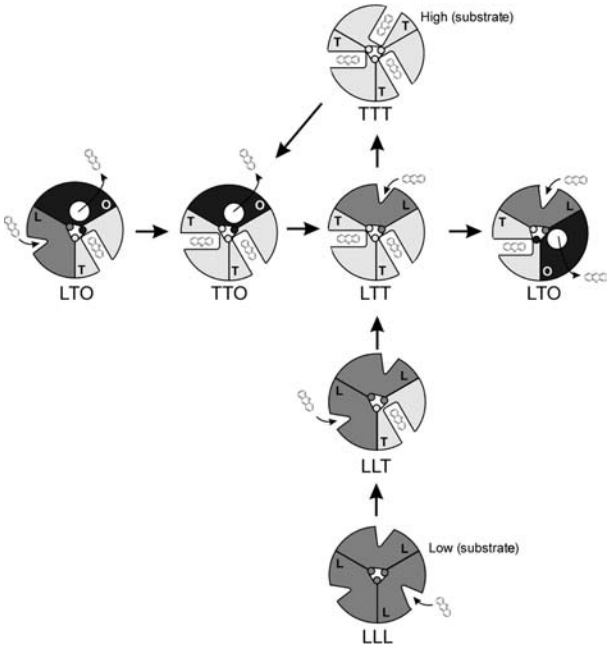

Figure 3 Schematic representation of the AcrB binding change functional rotation transport mechanism.
The conformational states loose (L), tight (T) and open (O) are indicated in different levels of gray. The lateral grooves in the L and T monomer indicate the substrate binding sites. The different geometric forms reflect low (triangle), high (rectangle) or no (circle) binding affinity for the transported substrates. State TTT is postulated to occur at high substrate concentration. The states LLL and LLT are postulated to occur in the absence or at low substrate concentrations. In this model, bi-site activation is essential for the complete transport cycle [adapted from Pos (2009) and modified].

(Figure 2). Substrate might enter the loose monomer via the TM8/TM9 groove (Murakami et al., 2002; Seeger et al., 2008a; Pos, 2009) or via tunnel 2 approximately 15 Å above the membrane plane. While it is not clear how hydrophobic compounds might enter tunnel 2 once these have been partitioned in the inner membrane, several groups provided structural data of symmetric AcrB (where all the monomers adopt the loose conformation) based on 3.2–3.8 Å data with presumably bound AcrB substrates in the tunnel 2 region (Yu et al., 2005; Drew et al., 2008). High resolution (2.5 Å) data describing the asymmetric trimer show clear densities in the TM8/TM9 groove of the loose monomer, which has been attributed to the highly concentrated detergent and AcrB substrate n-dodecyl-β-D-maltoside (Sennhauser et al., 2007). Upon conformational change from the loose to the tight state, tunnel 1 appears and might provide one of the pathways for substrates towards the hydrophobic pocket which accommodates the substrate molecule. Structural flexibility within the trimer (Takatsuka and Nikaido, 2007; Seeger et al., 2008b) suggests that the loose and even tight conformational states might be adoptable in the absence of substrates and that substrate binding to the hydrophobic pocket specifically stabilizes the tight conformation. This might also present an alternative role for tunnel 2 in these conformations as an exit pathway for compounds which are not substrates of the pump (Figure 2). In analogy with the binding change mechanism (Milgrom et al., 1998), the conversion of the tight monomer to the open monomer is energy-consuming and subject to bi-site activation, i.e., only occurs upon binding of substrate to the neighboring monomer (Figure 3). Upon transition from the tight to the open state, the binding pocket closes again; substrate is squeezed out and follows a newly formed tunnel (tunnel 3) to the TolC-docking domain funnel, and is from there finally extruded into the media via TolC.

In summary, upon conformational change from loose to tight to open and back to loose, an alternating access tunnel is formed through which substrates are transported from the outer leaflet of the inner membrane towards the outside medium. The mode of action is suggested to be based on occlusions migrating from the lateral entrance(s) to the central funnel and is reminiscent of a peristaltic pump.

To test the proposed conformational cycling *in vivo*, subdomains that undergo substantial rearrangement during cycling were locked by the introduction of disulfide bonds (Takatsuka and Nikaido, 2007; Seeger et al., 2008b). As could be demonstrated by tracing the efflux of a fluorescent substrate, formation of disulfide bonds significantly decreased AcrB mediated transport. When the disulfide bonds were broken by the addition of the reducing reagent dithiothreitol, transport activity was restored, which was in strong support of the functional rotation mechanism. Even more convincing, Takatsuka and Nikaido designed a functional covalently linked AcrB trimer, which could be inactivated by the introduction of a mutation in the proton relay network (D407A) or by disulfide formation in only *one* of the protomers (Takatsuka and Nikaido, 2009). These results are in accordance with the proposed functional rotation mechanism. More-

over, using quantitative measurements with β-lactams as substrates, Nagano and Nikaido (2009) found positive cooperativity for cephalosporins with low apparent affinity to AcrB (but not for nitrocefin, a cephalosporin with high affinity), which might indicate bi-site activation as postulated (Seeger et al., 2008a; Pos, 2009).

The interaction between each AcrB monomer and its affiliated AcrA molecule has been investigated very recently (Symmons et al., 2009) and might suggest that during functional rotation of AcrB subtle conformational changes are transmitted towards AcrA. Rather than just being a rigid adapter, AcrA might actively transduce energy generated by AcrB and induce subtle peristaltic motions in the TolC channel. Similar to the tunnels observed in a single AcrB protomer during functional rotation (Murakami et al., 2006; Seeger et al., 2006; Sennhauser et al., 2007), TolC is possibly not a rigid hollow cylinder but changes its diameter by conformational change of each monomer, thereby pushing substrate unidirectionally from the closing aperture into the media (Vaccaro et al., 2006, 2008; Seeger et al., 2008a; Pos, 2009).

Proton transport and energy transduction

AcrB utilizes the proton motive force to energize the extrusion of its cognate substrates from the cell into the medium (Zgurskaya and Nikaido, 1999; Saier and Paulsen, 2001). The TM domain of AcrB harbors four functionally essential charged residues that are conserved throughout the HAE-1 family: Asp407, Asp408, Lys940 and Arg971 (Su et al., 2006; Takatsuka and Nikaido, 2006). Another highly conserved TM residue, Thr978, is in hydrogen bonding distance from Asp407 in the loose and tight monomer and with Lys940 in the open monomer. However, when Thr978 was replaced by valine, isoleucine, leucine or asparagine, the relative activity of these mutants remained 40% to 60% as revealed by drug susceptibility assays (Takatsuka and Nikaido, 2006).

In the asymmetric structure of AcrB, the four above-mentioned essential residues Asp407, Asp408, Lys940 and Arg971 have distinct different conformations in at least one of the three conformers loose, tight and open (Murakami et al., 2006; Seeger et al., 2006; Sennhauser et al., 2007). Both structural and mutagenesis studies suggest that proton translocation is mediated by these titratable residues. The conformational changes during the putative conformational cycling in the TM domain are much more subtle compared to the porter domain: Lys940 is sandwiched between Asp407 and Asp408 in the loose and tight states, but becomes reoriented towards Thr978 in the open state; the N-terminal end of TM8 in the loose and tight monomers is marked by Pro874, but becomes elongated by four full turns in the open monomer, whereas TM5 bulges towards TM4 and TM10 in the open conformation. These conformational changes are thought to be the result of protonation and deprotonation events on these titratable, membrane embedded residues. The geometry of the titratable residues is reminiscent to the situation observed in bacteriorhodopsin, an archaeal integral membrane protein intensively studied since its discovery in the early seventies (Oesterhelt and Stoeckenius, 1973). It is therefore tempting to look for analogies between AcrB and the well-characterized bacteriorhodopsin. How these conformational changes are levered to the porter domain and cause the large conformational changes observed there is subject to ongoing investigation.

Acknowledgments

I would like to thank Markus Seeger and my collaborators at the University of Konstanz, Kay Diederichs and André Schiefner, for their indispensable efforts on this work.

References

Baev, N., Endre, G., Petrovics, G., Banfalvi, Z., and Kondorosi, A. (1991). Six nodulation genes of nod box locus 4 in *Rhizobium meliloti* are involved in nodulation signal production: nodM codes for D-glucosamine synthetase. Mol. Gen. Genet. *228*, 113–124.

Bavro, V.N., Pietras, Z., Furnham, N., Perez-Cano, L., Fernandez-Recio, J., Pei, X.Y., Misra, R., and Luisi, B. (2008). Assembly and channel opening in a bacterial drug efflux machine. Mol. Cell *30*, 114–121.

Bohnert, J.A., Schuster, S., Seeger, M.A., Fahnrich, E., Pos, K.M., and Kern, W.V. (2008). Site-directed mutagenesis reveals putative substrate binding residues in the *Escherichia coli* RND efflux pump AcrB. J. Bacteriol. *190*, 8225–8229.

Boyer, P.D. (1997). The ATP synthase – a splendid molecular machine. Annu. Rev. Biochem. *66*, 717–749.

Camacho, L.R., Constant, P., Raynaud, C., Laneelle, M.A., Triccas, J.A., Gicquel, B., Daffe, M., and Guilhot, C. (2001). Analysis of the phthiocerol dimycocerosate locus of *Mycobacterium tuberculosis*. Evidence that this lipid is involved in the cell wall permeability barrier. J. Biol. Chem. *276*, 19845–19854.

Davies, J.P. and Ioannou, Y.A. (2000). Topological analysis of Niemann-Pick C1 protein reveals that the membrane orientation of the putative sterol-sensing domain is identical to those of 3-hydroxy-3-methylglutaryl-CoA reductase and sterol regulatory element binding protein cleavage-activating protein. J. Biol. Chem. *275*, 24367–24374.

Davies, J.P., Chen, F.W., and Ioannou, Y.A. (2000). Transmembrane molecular pump activity of Niemann-Pick C1 protein. Science *290*, 2295–2298.

Domenech, P., Reed, M.B., and Barry, C.E., III. (2005). Contribution of the *Mycobacterium tuberculosis* MmpL protein family to virulence and drug resistance. Infect. Immun. *73*, 3492–3501.

Drew, D., Klepsch, M.M., Newstead, S., Flaig, R., De Gier, J.W., Iwata, S., and Beis, K. (2008). The structure of the efflux pump AcrB in complex with bile acid. Mol. Membr. Biol. *25*, 677–682.

Eda, S., Maseda, H., and Nakae, T. (2003). An elegant means of self-protection in Gram-negative bacteria by recognizing and extruding xenobiotics from the periplasmic space. J. Biol. Chem. *278*, 2085–2088.

Elkins, C.A. and Nikaido, H. (2002). Substrate specificity of the RND-type multidrug efflux pumps AcrB and AcrD of *Escherichia coli* is determined predominantly by two large periplasmic loops. J. Bacteriol. *184*, 6490–6498.

Gardel, C., Benson, S., Hunt, J., Michaelis, S., and Beckwith, J. (1987). secD, a new gene involved in protein export in *Escherichia coli*. J. Bacteriol. *169*, 1286–1290.

Guan, L. and Nakae, T. (2001). Identification of essential charged residues in transmembrane segments of the multidrug transporter MexB of *Pseudomonas aeruginosa*. J. Bacteriol. *183*, 1734–1739.

Hackney, D.D., Rosen, G., and Boyer, P.D. (1979). Subunit interaction during catalysis: alternating site cooperativity in photophosphorylation shown by substrate modulation of [^{18}O]ATP species formation. Proc. Natl. Acad. Sci. USA *76*, 3646–3650.

Hancock, R.E. and Brinkman, F.S. (2002). Function of pseudomonas porins in uptake and efflux. Annu. Rev. Microbiol. *56*, 17–38.

Hooper, D.C. (1995). Bacterial resistance to fluoroquinolones: mechanisms and patterns. Adv. Exp. Med. Biol. *390*, 49–57.

Hutton, R.L. and Boyer, P.D. (1979). Subunit interaction during catalysis. Alternating site cooperativity of mitochondrial adenosine triphosphatase. J. Biol. Chem. *254*, 9990–9993.

Infante, R.E., Abi-Mosleh, L., Radhakrishnan, A., Dale, J.D., Brown, M.S., and Goldstein, J.L. (2008a). Purified NPC1 protein. I. Binding of cholesterol and oxysterols to a 1278-amino acid membrane protein. J. Biol. Chem. *283*, 1052–1063.

Infante, R.E., Radhakrishnan, A., Abi-Mosleh, L., Kinch, L.N., Wang, M.L., Grishin, N.V., Goldstein, J.L., and Brown, M.S. (2008b). Purified NPC1 protein: II. Localization of sterol binding to a 240-amino acid soluble luminal loop. J. Biol. Chem. *283*, 1064–1075.

Ioannou, Y.A. (2001). Multidrug permeases and subcellular cholesterol transport. Nat. Rev. Mol. Cell Biol. *2*, 657–668.

Li, X.Z. and Nikaido, H. (2004). Efflux-mediated drug resistance in bacteria. Drugs *64*, 159–204.

Lomovskaya, O. and Totrov, M. (2005). Vacuuming the periplasm. J. Bacteriol. *187*, 1879–1883.

Lomovskaya, O., Lee, A., Hoshino, K., Ishida, H., Mistry, A., Warren, M.S., Boyer, E., Chamberland, S., and Lee, V.J. (1999). Use of a genetic approach to evaluate the consequences of inhibition of efflux pumps in *Pseudomonas aeruginosa*. Antimicrob. Agents Chemother. *43*, 1340–1346.

Mahamoud, A., Chevalier, J., Alibert-Franco, S., Kern, W.V., and Pages, J.M. (2007). Antibiotic efflux pumps in Gram-negative bacteria: the inhibitor response strategy. J. Antimicrob. Chemother. *59*, 1223–1229.

Mao, W., Warren, M.S., Black, D.S., Satou, T., Murata, T., Nishino, T., Gotoh, N., and Lomovskaya, O. (2002). On the mechanism of substrate specificity by resistance nodulation division (RND)-type multidrug resistance pumps: the large periplasmic loops of MexD from *Pseudomonas aeruginosa* are involved in substrate recognition. Mol. Microbiol. *46*, 889–901.

Mazzariol, A., Tokue, Y., Kanegawa, T.M., Cornaglia, G., and Nikaido, H. (2000). High-level fluoroquinolone-resistant clinical isolates of *Escherichia coli* overproduce multidrug efflux protein AcrA. Antimicrob. Agents Chemother. *44*, 3441–3443.

Milgrom, Y.M., Murataliev, M.B., and Boyer, P.D. (1998). Bi-site activation occurs with the native and nucleotide-depleted mitochondrial F1-ATPase. Biochem. J. *330*, 1037–1043.

Murakami, S. (2008). Multidrug efflux transporter, AcrB – the pumping mechanism. Curr. Opin. Struct. Biol. *18*, 459–465.

Murakami, S., Nakashima, R., Yamashita, E., and Yamaguchi, A. (2002). Crystal structure of bacterial multidrug efflux transporter AcrB. Nature *419*, 587–593.

Murakami, S., Nakashima, R., Yamashita, E., Matsumoto, T., and Yamaguchi, A. (2006). Crystal structures of a multidrug transporter reveal a functionally rotating mechanism. Nature *443*, 173–179.

Murray, D.S., Schumacher, M.A., and Brennan, R.G. (2004). Crystal structures of QacR-diamidine complexes reveal additional multidrug-binding modes and a novel mechanism of drug charge neutralization. J. Biol. Chem. *279*, 14365–14371.

Nagano, K. and Nikaido, H. (2009). Kinetic behavior of the major multidrug efflux pump AcrB of *Escherichia coli*. Proc. Natl. Acad. Sci. USA *106*, 5854–5858.

Nakano, Y., Kim, H.R., Kawakami, A., Roy, S., Schier, A.F., and Ingham, P.W. (2004). Inactivation of dispatched 1 by the chameleon mutation disrupts Hedgehog signalling in the zebrafish embryo. Dev. Biol. *269*, 381–392.

Nikaido, H. (1996). Multidrug efflux pumps of Gram-negative bacteria. J. Bacteriol. *178*, 5853–5859.

Nikaido, H. (1998). Multiple antibiotic resistance and efflux. Curr. Opin. Microbiol. *1*, 516–523.

Nikaido, H. (2003). Molecular basis of bacterial outer membrane permeability revisited. Microbiol. Mol. Biol. Rev. *67*, 593–656.

Nikaido, H. (2009). Multidrug resistance in bacteria. Annu. Rev. Biochem. *78*, 119–146.

Nikaido, H. and Takatsuka, Y. (2008). Mechanisms of RND multidrug efflux pumps. Biochim. Biophys. Acta *1794*, 769–781.

Oesterhelt, D. and Stoeckenius, W. (1973). Functions of a new photoreceptor membrane. Proc. Natl. Acad. Sci. USA *70*, 2853–2857.

Pietras, Z., Bavro, V.N., Furnham, N., Pellegrini-Calace, M., Milner-White, E.J., and Luisi, B.F. (2008). Structure and mechanism of drug efflux machinery in Gram-negative bacteria. Curr. Drug Targets *9*, 719–728.

Plesiat, P. and Nikaido, H. (1992). Outer membranes of Gram-negative bacteria are permeable to steroid probes. Mol. Microbiol. *6*, 1323–1333.

Pogliano, J.A. and Beckwith, J. (1994). SecD and SecF facilitate protein export in *Escherichia coli*. EMBO J. *13*, 554–561.

Pos, K.M. (2009). Drug transport mechanism of the AcrB efflux pump. Biochim. Biophys. Acta *1794*, 782–793.

Pos, K.M., Schiefner, A., Seeger, M.A., and Diederichs, K. (2004). Crystallographic analysis of AcrB. FEBS Lett. *564*, 333–339.

Saier, M.H., Jr. and Paulsen, I.T. (2001). Phylogeny of multidrug transporters. Semin. Cell Dev. Biol. *12*, 205–213.

Schumacher, M.A., Miller, M.C., Grkovic, S., Brown, M.H., Skurray, R.A., and Brennan, R.G. (2001). Structural mechanisms of QacR induction and multidrug recognition. Science *294*, 2158–2163.

Schumacher, M.A., Miller, M.C., and Brennan, R.G. (2004). Structural mechanism of the simultaneous binding of two drugs to a multidrug-binding protein. EMBO J. *23*, 2923–2930.

Seeger, M.A., Schiefner, A., Eicher, T., Verrey, F., Diederichs, K., and Pos, K.M. (2006). Structural asymmetry of AcrB trimer suggests a peristaltic pump mechanism. Science *313*, 1295–1298.

Seeger, M.A., Diederichs, K., Eicher, T., Brandstatter, L., Schiefner, A., Verrey, F., and Pos, K.M. (2008a). The AcrB efflux pump: conformational cycling and peristalsis lead to multidrug resistance. Curr. Drug Targets *9*, 729–749.

Seeger, M.A., von Ballmoos, C., Eicher, T., Brandstatter, L., Verrey, F., Diederichs, K., and Pos, K.M. (2008b). Engineered disulfide bonds support the functional rotation mechanism of multidrug efflux pump AcrB. Nat. Struct. Mol. Biol. *15*, 199–205.

Sennhauser, G., Amstutz, P., Briand, C., Storchenegger, O., and Grutter, M.G. (2007). Drug export pathway of multidrug exporter AcrB revealed by DARPin inhibitors. PLoS Biol. *5*, e7.

Skinner, R., Cundliffe, E., and Schmidt, F.J. (1983). Site of action of a ribosomal RNA methylase responsible for resistance to erythromycin and other antibiotics. J. Biol. Chem. *258*, 12702–12706.

Sleat, D.E., Wiseman, J.A., El-Banna, M., Price, S.M., Verot, L., Shen, M.M., Tint, G.S., Vanier, M.T., Walkley, S.U., and Lobel, P. (2004). Genetic evidence for nonredundant functional cooperativity between NPC1 and NPC2 in lipid transport. Proc. Natl. Acad. Sci. USA *101*, 5886–5891.

Su, C.C., Li, M., Gu, R., Takatsuka, Y., McDermott, G., Nikaido, H., and Yu, E.W. (2006). Conformation of the AcrB multidrug efflux pump in mutants of the putative proton relay pathway. J. Bacteriol. *188*, 7290–7296.

Symmons, M.F., Bokma, E., Koronakis, E., Hughes, C., and Koronakis, V. (2009). The assembled structure of a complete tripartite bacterial multidrug efflux pump. Proc. Natl. Acad. Sci. USA *106*, 7173–7178.

Taipale, J., Cooper, M.K., Maiti, T., and Beachy, P.A. (2002). Patched acts catalytically to suppress the activity of Smoothened. Nature *418*, 892–897.

Takatsuka, Y. and Nikaido, H. (2006). Threonine-978 in the transmembrane segment of the multidrug efflux pump AcrB of *Escherichia coli* is crucial for drug transport as a probable component of the proton relay network. J. Bacteriol. *188*, 7284–7289.

Takatsuka, Y. and Nikaido, H. (2007). Site-directed disulfide cross-linking shows that cleft flexibility in the periplasmic domain is needed for the multidrug efflux pump AcrB of *Escherichia coli*. J. Bacteriol. *189*, 8677–8684.

Takatsuka, Y. and Nikaido, H. (2009). Covalently linked trimer of the AcrB multidrug efflux pump provides support for the functional rotating mechanism. J. Bacteriol. *191*, 1729–1737.

Tamura, N., Murakami, S., Oyama, Y., Ishiguro, M., and Yamaguchi, A. (2005). Direct interaction of multidrug efflux transporter AcrB and outer membrane channel TolC detected via site-directed disulfide cross-linking. Biochemistry *44*, 11115–11121.

Thomson, K.S. and Smith Moland, E. (2000). Version 2000: the new β-lactamases of Gram-negative bacteria at the dawn of the new millennium. Microbes Infect. *2*, 1225–1235.

Tikhonova, E.B. and Zgurskaya, H.I. (2004). AcrA, AcrB, and TolC of *Escherichia coli* form a stable intermembrane multidrug efflux complex. J. Biol. Chem. *279*, 32116–32124.

Tornroth-Horsefield, S., Gourdon, P., Horsefield, R., Brive, L., Yamamoto, N., Mori, H., Snijder, A., and Neutze, R. (2007). Crystal structure of AcrB in complex with a single transmembrane subunit reveals another twist. Structure *15*, 1663–1673.

Vaccaro, L., Koronakis, V., and Sansom, M.S. (2006). Flexibility in a drug transport accessory protein: molecular dynamics simulations of MexA. Biophys. J. *91*, 558–564.

Vaccaro, L., Scott, K.A., and Sansom, M.S. (2008). Gating at both ends and breathing in the middle: conformational dynamics of TolC. Biophys. J. *95*, 5681–5691.

Wright, G.D. (1999). Aminoglycoside-modifying enzymes. Curr. Opin. Microbiol. *2*, 499–503.

Yoshida, H., Bogaki, M., Nakamura, M., and Nakamura, S. (1990). Quinolone resistance-determining region in the DNA gyrase gyrA gene of *Escherichia coli*. Antimicrob. Agents Chemother. *34*, 1271–1272.

Yu, E.W., Aires, J.R., and Nikaido, H. (2003a). AcrB multidrug efflux pump of *Escherichia coli*: composite substrate-binding cavity of exceptional flexibility generates its extremely wide substrate specificity. J. Bacteriol. *185*, 5657–5664.

Yu, E.W., McDermott, G., Zgurskaya, H.I., Nikaido, H., and Koshland, D.E., Jr. (2003b). Structural basis of multiple drug-binding capacity of the AcrB multidrug efflux pump. Science *300*, 976–980.

Yu, E.W., Aires, J.R., McDermott, G., and Nikaido, H. (2005). A periplasmic drug-binding site of the AcrB multidrug efflux pump: a crystallographic and site-directed mutagenesis study. J. Bacteriol. *187*, 6804–6815.

Zalacain, M. and Cundliffe, E. (1989). Methylation of 23S rRNA caused by tlrA (ermSF), a tylosin resistance determinant from *Streptomyces fradiae*. J. Bacteriol. *171*, 4254–4260.

Zalacain, M. and Cundliffe, E. (1990). Methylation of 23S ribosomal RNA due to carB, an antibiotic-resistance determinant from the carbomycin producer, *Streptomyces thermotolerans*. Eur. J. Biochem. *189*, 67–72.

Zgurskaya, H.I. and Nikaido, H. (1999). Bypassing the periplasm: reconstitution of the AcrAB multidrug efflux pump of *Escherichia coli*. Proc. Natl. Acad. Sci. USA *96*, 7190–7195.

Zheleznova, E.E., Markham, P.N., Neyfakh, A.A., and Brennan, R.G. (1999). Structural basis of multidrug recognition by BmrR, a transcription activator of a multidrug transporter. Cell *96*, 353–362.

Received March 1, 2009; accepted April 29, 2009